R. & M. No. 3190
(18,072)
A.R.C. Technical Report

MINISTRY OF AVIATION

AERONAUTICAL RESEARCH COUNCIL
REPORTS AND MEMORANDA

Some Observations of the Flow over a Delta-Winged Model with 55-deg Leading-Edge Sweep, at Mach Numbers between 0·4 and 1·8

By

E. P. SUTTON, M.A.

LONDON: HER MAJESTY'S STATIONERY OFFICE
1960
PRICE 10*s*. 6*d*. NET

Some Observations of the Flow over a Delta-Winged Model with 55-deg Leading-Edge Sweep, at Mach Numbers between 0·4 and 1·8

By

E. P. Sutton, M.A.

Communicated by the Principal Director of Scientific Research (Air), Ministry of Supply

Reports and Memoranda No. 3190*

November, 1955

Summary.—A delta-winged model, with 54·8-deg leading-edge sweep and a 6 per cent thick RAE 101 section, has been tested in the Royal Aeronautical Establishment (Bedford) 3-ft Wind Tunnel. The results of lift and pitching-moment measurements at Mach numbers from 0·70 to 1·02 and from 1·42 to 1·82 are presented and discussed with the aid of surface oil-flow observations. The Reynolds number of the tests was between 2·2 and $3 \cdot 3 \times 10^6$.

At Mach numbers up to at least 1·07 a leading-edge-separation vortex sheet formed on the wing at incidence. An interaction between the vortex sheet and the wing upper-surface shock wave at Mach numbers just below 1·0 caused unsteadiness of the forces on the model and a pitch-up. At Mach numbers from 1·42 to 1·82 the flow was attached at the leading edge, and an oblique shock lay across the upper surface of the wing.

1. *Introduction.*—As part of an investigation of the effects of plan-form on the aerodynamic characteristics of wings at transonic and supersonic speeds, a delta-winged model with leading-edge sweep 54·8 deg was tested in the Royal Aircraft Establishment (Bedford) 3-ft Wind Tunnel. The wing plan-form was one of a systematic series proposed by Warren in an unpublished Royal Aircraft Establishment memorandum.

The present paper has been written to provide a summary of the results of lift and pitching-moment measurements, with particular attention to the effects of flow separations detected by visual observations of the flow of oil on the wing. The lift, stability and surface flow at a Mach number of 0·8 are first discussed in some detail. With these as a basis, the effects of increasing Mach number are considered, beginning with a brief analysis of the results obtained at a Mach number of 0·96. Finally, the characteristics of the model at supersonic speeds are described.

A Table of lift and pitching-moment coefficients is included.

2. *Description of the Model and of the Tests.*—The main dimensions of the model are given in Fig. 1. It consisted of a delta wing of leading-edge sweep 54·8 deg with a symmetrical 6 per cent thick RAE 101 section mounted on the cylindrical part of an ogive-cylinder body. The extreme tips of the wing had been removed, giving a taper ratio of 0·01 ; the aspect ratio of the model was 2·76, compared with 2·83 for the full delta wing.

* R.A.E. Tech. Note Aero 2430, received 11th January, 1956.

The wing was made of high-tensile stainless steel, and the body partly of steel and partly of aluminium alloy, to a high standard of surface finish. Except where otherwise stated, the leading edges of the wing had been roughened by the application of a mixture of fine carborundum powder in aluminium paint in a band extending from 10 per cent local chord on the lower surface to 10 per cent chord on the upper surface. In the transonic tests the band had a base of paint about $0 \cdot 001$ in. thick out of which the carborundum grains (Grade F) formed projections about $0 \cdot 0015$ in. high. For the supersonic tests a coarser powder (Grade 240) was used, making the height of the projections about $0 \cdot 0025$ in. The boundary layer on the body was made turbulent ahead of the wings for all of the tests by means of a wire of diameter $0 \cdot 005$ in. at a distance of $2 \cdot 5$ in. from the nose.

The tests were made in the R.A.E. (Bedford) 3-ft Wind Tunnel[1,2], at Mach numbers between $0 \cdot 40$ and $1 \cdot 02$ in the 35-in. by 27-in. slotted-wall transonic working-section, and at Mach numbers of $1 \cdot 42$, $1 \cdot 61$ and $1 \cdot 82$ in the 36-in. square supersonic working-section. The Reynolds number based on the aerodynamic mean chord was $2 \cdot 2 \times 10^6$ at a Mach number of $0 \cdot 40$ (surface oil flow observation only), $3 \cdot 3 \times 10^6$ at Mach numbers from $0 \cdot 70$ to $1 \cdot 02$, $2 \cdot 7 \times 10^6$ at Mach numbers of $1 \cdot 42$ and $1 \cdot 61$, and $2 \cdot 4 \times 10^6$ at a Mach number of $1 \cdot 82$.

The model was mounted on a sting. An internal strain-gauge balance was used to measure the normal force and pitching moment at angles of incidence up to 14 deg, except at a Mach number of $1 \cdot 42$, where reflection of the bow wave of the model from the tunnel walls limited the incidence to 9 deg. For the reduction of normal force to lift, measurements of axial force were made using another balance, at angles of incidence up to 10 deg ; extrapolation was necessary at the higher incidences, and for Mach numbers of $1 \cdot 61$ and $1 \cdot 82$ some measurements of axial force with transition free were utilised. As the contribution of axial force to lift did not exceed $1 \cdot 2$ per cent, the error in these approximations is not significant. Measurements of base pressure were made and used to adjust the axial force to that for a base pressure equal to the static pressure of the undisturbed stream.

The experimental accuracy is estimated to have been :

Lift coefficient	$\pm 0 \cdot 005$
Pitching-moment coefficient	$\pm 0 \cdot 001$
Angle of incidence	$\pm 0 \cdot 1$ deg
Mach number	$\pm 0 \cdot 003$

No corrections have been applied for tunnel interference. An experimental investigation on another model shape in the transonic working-section has shown that interference effects are likely to be small at Mach numbers up to $0 \cdot 95$. At Mach numbers near 1 a negative blockage correction may be applicable, and the effective Mach number may be up to $0 \cdot 02$ less than the value quoted ; wall interference tends to delay the rearward movement of strong shocks on the model. It is also possible that a small upwash correction is needed throughout the subsonic and transonic range.

Observations were made by the surface oil-flow technique[3] to provide qualitative information about the nature of the flow over the wing at incidence. A thin film of heavy oil containing a suspension of titanium oxide, with a trace of oleic acid as anti-coagulant, was applied to the wing and exposed to the flow. The oil did not flow on the wing where the boundary layer was laminar, except in the high shear region near the leading edge. Where the boundary layer was turbulent the oil flowed in a direction which is presumed to approximate to that of the airflow in the lower part of the boundary layer. The experimental pattern should, therefore, be an approximation to the pattern of the limiting streamlines in the surface as discussed by Maskell[8]. The oil-flow pattern usually developed in about five minutes, after which the tunnel was stopped and the model photographed. Further details of the use of this technique and the interpretation of the results may be found in Ref. 4.

3. *Results and Discussion.*—The measured lift and pitching-moment coefficients are tabulated in Table 1. Curves of lift coefficient against incidence and of pitching-moment coefficient against lift coefficient are given in Figs. 2a and 3a respectively for Mach numbers of 0·70, 0·80, 0·90, 0·93 and 0·96, and in Figs. 2b and 3b for Mach numbers of 0·96, 0·99, 1·02, 1·42, 1·61 and 1·82. They are discussed in the following Sections.

Fig. 4 shows the variation with Mach number of the lift-curve slope and aerodynamic-centre position of the model at zero incidence.

In Figs. 6, 7, 8, 9 and 10, photographs of oil flow on the wings of the model at Mach numbers of 0·40, 0·80, 0·90 and 0·96, 0·99 and 1·61 respectively are reproduced. For convenience of reference in the discussion of the flow over the wings, the lift and pitching-moment coefficients at Mach numbers of 0·80 and 0·96 have been plotted again in Fig. 5, and the curves labelled with the identifying letters of the photographs in Figs. 7 and 8.

3.1. *Flow with Leading-Edge Separation, at a Mach Number of* 0·80.—The variation of lift coefficient with incidence and the variation of pitching-moment coefficient with lift coefficient at a Mach number of 0·80 are shown together in Fig. 5.

At this Mach number the lift-curve slope was constant, within the limits of experimental error, up to a lift coefficient of 0·34. With further increase in incidence there was a gradual decrease in lift-curve slope, continuing up to a lift coefficient of 0·54, beyond which there was a rapid recovery to about the original value. The slope of the curve of pitching-moment coefficient against lift coefficient was constant up to a lift coefficient of approximately 0·23, when a gradual reduction in longitudinal stability $(-\ \partial C_m/\partial C_L)_M$ began. There was a sharper loss of stability at lift coefficients near 0·45, followed quickly by a recovery. At lift coefficients from 0·55 to 0·75 the stability was almost constant, and greater than at low lift coefficients. The results of repeat tests did not agree completely at lift coefficients between 0·4 and 0·5, but differed in the strength of the pitch-up observed.

Photographs of surface oil flow at a Mach number of 0·8 are reproduced in Fig. 7. They show that the flow about the wing at incidence was one with a leading-edge vortex sheet[5, 6, 7, 8], the characteristics of which at low speeds will be stated briefly before the photographs are discussed.

A sketch of the main features of such a flow is given in Fig. 11, following Küchemann. The boundary layer separates at the leading edge to form a vortex sheet, the free edge of which rolls up above the upper surface of the wing. Main-stream air flows up and over the vortex sheet and is swept down again towards the wing surface. Streamlines such as AA flow under the vortex sheet with a large spanwise component of velocity and continue spirally downstream into the core of high vorticity formed by the rolling-up of the edge of the sheet. Streamlines such as BB which pass above the dividing stream-surface DD continue downstream over the wing in an approximately chordwise direction, inboard of the vortex sheet.

Beneath the vortex core formed by the rolled-up edge of the sheet the local suction on the wing surface is high. The new boundary layer formed by the outward surface flow encounters an adverse pressure gradient after passing the suction peak, and separates before it reaches the leading edge. A secondary coiled vortex sheet may be formed near the leading edge underneath the main sheet, or the angle between the wing surface and the main vortex sheet may be occupied by a separation bubble of relatively slow-moving air. The latter possibility is more consistent with the oil-flow observations reported here, and is the one illustrated in Fig. 11.

At moderate angles of incidence the vortex sheet is roughly conical in shape above the wing, with apex O on the leading edge. The rolled-up edge of the sheet remains close to the wing surface along a ray from O, lying in plan view between the leading edge and a line through O in the free-stream direction. At higher incidence the vortex core may lift farther away from the wing surface well ahead of the trailing edge, and trail downstream more nearly in the free-stream direction[9, 10]*.

* (January, 1960.) Some of the observations associated in the following discussion with a lifting-away of the vortex core from the wing surface may well be better interpreted in terms of the 'vortex breakdown' phenomenon, since reported by Peckham and Atkinson[15] and by others.

The surface pattern formed by the flow of oil on a wing with a leading-edge separation of this kind is illustrated by many examples in Ref. 9, and the general relation between the limiting flow pattern in the surface and the type of separation occurring in the three-dimensional flow is discussed in Ref. 8. A typical example from the present tests, reproduced in Fig. 12, shows the characteristic division of the pattern at moderate incidences into three distinct regions. Inboard of the dividing line OD, which is the attachment line of the surface flow that has passed over the vortex sheet, the oil flows mainly in the chordwise direction ; between OD and the secondary separation line OS, the oil flow is inclined outwards, towards the leading edge ; while between OS and the leading edge little movement of the oil has occurred. There is no flow across OD and OS ; the surface flow at these lines is along them, and the dividing line OD has the appearance of a locus of cusps[8]. As a rough guide, the projection of the vortex core on the wing may be taken to lie through the points of inflexion of the streamlines between OD and OS. The secondary separation line OS is often ill-defined because the oil flow towards it is relatively slow. In a number of the photographs reproduced in this paper, including Fig. 12, it is evident that the oil streamlines have not all reached their envelope along the separation line, as they would have done if the wing had been exposed longer to the flow.

The oil-flow photographs obtained at a Mach number of 0·80, presented in Figs. 7a to 7h, will now be described in relation to the variation of lift and pitching moment on the wing.

The observations were made with the leading edge of only one wing roughened, and that of the other smooth, allowing natural transition. The photographs of the smooth wing have been included here mainly as an aid to the interpretation of the photographs of the wing with roughened leading edge at lift coefficients between zero and 0·37 ; the lift and pitching moment on the wing in this range were identical, within the limits of experimental error, whether or not the leading edge was roughened. There were measurable but still small differences at the higher lift coefficients. All of the photographs are of the suction surface of the wing.

The oil pattern on the smooth wing in Fig. 7a shows that at zero incidence the boundary layer was laminar near the leading edge. Transition occurred at about two-thirds of the local chord over the outer part of the wing, except where individual disturbances near the leading edge caused earlier transition. Over the inboard half of the wing transition was due entirely to individual disturbances near the leading edge, and no clearly defined transition front was observed. (The leading edge of the model was known to have been pitted slightly by solid particles carried in the tunnel air stream.) The thick irregular line near the leading edge was merely an accumulation of oil pushed back from the region of maximum shear, moving back with time throughout the exposure to the flow.

On the roughened wing the boundary layer was turbulent everywhere behind the roughness band.

At a lift coefficient of 0·12 (Fig. 7b), a short-bubble leading-edge separation with turbulent re-attachment had appeared along the outer quarter of the span of the smooth wing. The evidence for this is the presence of a thin line of oil, downstream of which the boundary layer was turbulent, close to the leading edge in Fig. 7b ; this line is distinguishable by its chordwise position from the accumulation of oil driven back from the leading edge farther inboard. The flow on the wing with roughened leading edge was not visibly different from that at zero incidence.

Fig. 7c shows the surface oil flow at a lift coefficient of 0·25, just above that at which the force measurements first showed a reduction in stability (Fig. 5). On the outer third of the smooth wing the typical surface pattern of a flow with a leading-edge vortex sheet can be seen. Farther inboard, there was a short-bubble separation with turbulent re-attachment. (The oil line at the position of the separation bubble is somewhat obscured by the high lights in the photograph.)

On the outer part of the roughened wing, the surface flow had a strong spanwise component of velocity over an area roughly the same as that of the outward flow under the vortex sheet on the smooth wing, but was less regular. A similar surface flow pattern, suggesting an array of small vortices lying chordwise across the wing, has been observed by O'Hara and Scott-Wilson[4]. The difference between the patterns on the two wings in Fig. 7c persists in Fig. 7d, but has almost disappeared in Fig. 7e. It has not been fully explained. A leading-edge vortex sheet on the roughened wing may have rolled up in short sections to produce an array of streamwise vortices above the wing, but in such a way that the outflow and the loading on the wing were similar, on the whole, to those on the smooth wing. It will be assumed that the difference is not important here, and that the measured lift and pitching moment may be related to the simpler flow patterns on the smooth wing in Figs. 7c and 7d.

The results of low-speed tests on wings of a variety of plan-forms (in Ref. 9, for example), have shown that the main effects of a leading-edge vortex sheet with a rolled-up edge on the loading on the wing may be expected to be an increase in lift beneath the rolled-up edge, and a loss of lift farther outboard. Since at the incidence of Fig. 7c the aerodynamic centre was beginning to move forward without any measurable change in lift-curve slope, it is deduced that the loss of lift at the tips was approximately equal in magnitude to the gain in lift acting farther forward beneath the rolled-up edge of the vortex sheet (or its equivalent on the roughened wing).

Fig. 7d shows that at a lift coefficient of 0·37 the vortex sheet had spread inboard over about four-fifths of the leading edge, while the separation bubble had grown considerably at the tips. At this lift coefficient the lift-curve slope had begun to fall (Fig. 5), suggesting that the loss of lift near the tips now exceeded the gain farther inboard.

At a lift coefficient of 0·48 (Fig. 7e), the apex of the vortex sheet had reached the wing root. A further significant change is apparent in the oil-flow pattern in that the dividing line is no longer clearly defined right across the wing, but becomes obscure shortly after crossing the mid-chord line. It is probable that the rolled-up edge of the vortex sheet had lifted farther away from the wing surface downstream of the point at which the dividing line became indistinct. Such a change may be thought of as due to the increasing influence of the trailing edge on the otherwise roughly conical development of the vortex sheet.

The aerodynamic centre had continued to move forward between the lift coefficients of Figs. 7d and 7e. A loss of lift near the trailing edge of the outer part of the wing as the vortex core first lifted away from it may have contributed to this further decrease in stability, but the increase in lift on the forward part of the wing due to the movement of the apex of the vortex sheet to the root leading edge was probably mainly responsible.

With further increase in incidence (Figs. 7f, 7g and 7h), the point at which the dividing line became indistinct moved forward, and at the same time the whole surface flow pattern due to the vortex sheet moved inboard, turning about the root leading edge. The force measurements showed a large rearward shift of aerodynamic centre between a lift coefficient of 0·48 (Fig. 7e) and a lift coefficient of 0·52 (Fig. 7f), and an increase in lift-curve slope at lift coefficients in the neighbourhood of 0·57 (Fig. 7g). Apart from any effect of the increasing detachment of the vortex core from the rear part of the wing, a recovery of stability is to be expected once the apex of the vortex sheet reaches the root leading edge, and can no longer move forward with increasing lift coefficient. Inspection of the results of low-speed pressure-distribution measurements on delta wings[11,12] suggests that, in addition, the rate of growth of lift near the trailing edge of the wing increases again as the point at which the vortex core begins to lift farther away from the surface moves forward over the wing.

3.2. *Flow with Leading-Edge Separation Interacting with a Rear Shock, at a Mach Number of 0·96*.—Fig. 4 shows that at a Mach number of 0·96 the lift-curve slope at zero incidence was higher by about 30 per cent, and the aerodynamic centre was 7 per cent of the aerodynamic mean chord farther back, than at a Mach number of 0·80. This change in loading at low lift coefficients, before the onset of leading edge separation, is no doubt due in part to the development of regions of supersonic flow on the wing.

In Fig. 5 the variation of lift coefficient with incidence and of pitching-moment coefficient with lift coefficient at a Mach number of 0·96 may be compared with those at a Mach number of $0 \cdot 80$. The lift-curve slope began to fall at a lift coefficient of about $0 \cdot 25$ at $0 \cdot 96$, compared with $0 \cdot 34$ at $0 \cdot 80$, while the lift coefficient at which the aerodynamic centre began to move forward was about the same, $0 \cdot 23$, at both Mach numbers.

Two successive reductions in stability were observed at a Mach number of $0 \cdot 96$. The first was followed by a partial recovery at lift coefficients between $0 \cdot 4$ and $0 \cdot 45$. The aerodynamic-centre position then remained constant until the second forward movement began at a lift coefficient of about $0 \cdot 6$; this was followed by a recovery in stability at lift coefficients between $0 \cdot 7$ and $0 \cdot 75$ to a slightly higher value than that at low incidence. The lift-curve slope was approximately constant at lift coefficients between $0 \cdot 3$ and $0 \cdot 6$; it decreased at lift coefficients between $0 \cdot 6$ and $0 \cdot 7$ and then began to increase again. The lift and pitching moment on the model were observed to be very unsteady at lift coefficients greater than $0 \cdot 6$.

Photographs of surface oil flows at Mach numbers of $0 \cdot 90$ and $0 \cdot 96$ are reproduced in Figs. 8a to 8c. A small indentation into the region of outward flow on the surface will be seen in each photograph, indicating an early local separation of the boundary layer of the flow approaching the leading edge beneath the vortex sheet. This appears to have been due to the presence of a shock which extended across the wing, at least in the region between the dividing lines. This would affect the pressure field and hence distort the spiral flow around the coiled vortex sheets. Direct evidence of the existence of the shock is to be found in changes of surface flow direction inboard of the dividing line ; they can be seen clearly in Figs. 8a and 8c if the oil pattern is viewed along the streamlines. The broken lines in the sketches accompanying the photographs have been drawn through the local separations and the narrow bands in which the streamlines inboard of the dividing line changed direction, to show roughly the presumed position of the shock. (In the case of Fig. 8b the pattern on the other wing of the model with smooth leading edge showed the deflection of the streamlines more clearly.) No attempt has been made to depict its interaction with the vortex sheet in detail. It is evident from the photographs that the rolled-up edge of the sheet was deflected away from the wing ; the end of the well-defined dividing line of the surface flow was always close to the apparent shock position*.

The shock moved forward over the wing with increasing angle of incidence at constant Mach number (Figs. 8b and 8c), and back with increasing Mach number at constant incidence (Figs. 8a and 8c).

Returning to the force measurements at a Mach number of $0 \cdot 96$, the reason why the aerodynamic-centre position remained constant at lift coefficients between $0 \cdot 5$ and $0 \cdot 6$ appears to be that the leading-edge vortex sheet continued to maintain its conical shape almost to the trailing edge, after the apex had reached the wing root. The modifying influence of the trailing edge on the development of the vortex sheet would be expected to be delayed to higher lift coefficients than at a Mach number of $0 \cdot 8$ by the presence of a region of supersonic flow above the wing. The second forward movement of the aerodynamic centre and reduction in lift-curve slope, and the subsequent recovery, were associated with the forward movement of the shock from the trailing edge and the lifting of the vortex core away from the wing surface.

3.3. *Lift and Stability at Mach Numbers between* $0 \cdot 4$ *and* $1 \cdot 02$.—A photograph of the surface oil flow at an angle of incidence of $10 \cdot 3$ deg at a Mach number of $0 \cdot 40$, which was the lowest Mach number at which any observations were made, is reproduced in Fig. 6. The apex of the vortex sheet on the roughened wing had almost reached the root leading edge, and the dividing line of the surface flow did not extend quite to the trailing edge. The state of development of the vortex sheet was a little less advanced than that at an angle of incidence of $8 \cdot 6$ (Fig. 7e) at a Mach number of $0 \cdot 80$. (At constant Mach number, the difference between the Reynolds numbers of the tests at Mach numbers of $0 \cdot 40$ and $0 \cdot 80$ would be expected to have the opposite effect to that observed. The vortex sheet would develop more rapidly at the lower Reynolds number.) No force measurements were made at a Mach number of $0 \cdot 40$.

---

* (January, 1960.) *See* footnote to Section 3.1, para. 6.

Force measurements at a Mach number of 0·70 gave lift and pitching-moment curves (Figs. 2a and 3a) which differed only slightly from those at a Mach number of 0·80. A feature of the shape of the lift curve which should be noted was the increase in lift-curve slope at a lift coefficient of about 0·2 ; no such increase was observed at higher Mach numbers.

The lift coefficient at which the lift-curve slope began to decrease was about 0·39 at a Mach number of 0·70, compared with 0·34 at a Mach number of 0·80 ; the lift coefficient at which the aerodynamic centre began to move forward was about the same at both Mach numbers.

The trend of reduction with increasing Mach number in the lift coefficient at which the lift-curve slope began to decrease continued up to a Mach number of 0·96. This is consistent with the development suggested by the surface oil-flow observations at Mach numbers of 0·40 and 0·80 : the higher the Mach number, the more rapidly the leading-edge separation spread inboard with increasing incidence.

At still higher Mach numbers (Fig. 2b) the lift coefficient at which the reduction in lift-curve slope began increased again, from 0·25 at a Mach number of 0·96 to 0·33 at a Mach number of 1·02.

The lift coefficients at which the steeper loss of stability and subsequent recovery occurred increased with Mach number up to 0·99 (Figs. 3a and 3b), while at 1·02 there was relatively little variation in stability at the higher lift coefficients of the tests. It was suggested in the previous Section that this effect of increasing Mach number was due to a reduction in the influence of the trailing edge on the shape of the vortex sheet at the higher lift coefficients as the supersonic flow over the upper surface of the wing developed.

At a Mach number of 0·99 there were large fluctuations in the balance readings at all lift coefficients above about 0·6, and the results were not accurately repeatable. There was a very abrupt loss of lift (Fig. 2b) and nose-up change in pitching moment (Fig. 3b), at a lift coefficient just below 0·9. Photographs of oil flow on the wing at lift coefficients of 0·65, 0·83 and 0·86 (after the pitch-up) are given in Figs. 9a to 9c. At lift coefficients of 0·65 and 0·83 the shock position on the wing surface was near the trailing edge, and the rolled-up edge of the vortex sheet remained close to the wing surface. The pitch-up coincided with the forward movement of the shock and detachment of the vortex core from the proximity of the wing near the trailing edge ; intermittent movement of the shock was probably responsible also for the unsteadiness at lower lift coefficients.

At a Mach number of 1·02 the balance readings were steady again. After a partial recovery of stability at lift coefficients between 0·5 and 0·6 there was a small further loss, accompanied by a reduction in lift-curve slope, at a lift coefficient of about 0·7. There was no sudden loss of lift within the incidence range of the tests, but it is possible that a sudden forward movement of the shock from the trailing edge, similar to that at a Mach number of 0·99, would occur at a higher lift coefficient at a Mach number of 1·02.

An oil-flow observation, not reproduced, showed that there was still a leading-edge vortex sheet at a Mach number of 1·07 at an angle of incidence of 12 deg. No tests were done at Mach numbers between 1·07 and 1·42.

3.4. *Lift and Stability and the Flow on the Wing at Mach Numbers from* 1·42 to 1·82.—Figs. 2b and 3b show that the variations with lift coefficient of the lift-curve slope and aerodynamic-centre position at Mach numbers of 1·42, 1·61 and 1·82 were smaller and smoother on the whole than at subsonic speeds. There was a slight reduction in lift-curve slope at lift coefficients between 0·35 and 0·45 at all three Mach numbers, and a forward movement of aerodynamic centre at lift coefficients in the neighbourhood of 0·35 at a Mach number of 1·42, 0·25 at 1·61, and 0·15 at 1·82 ; a further reduction in stability occurred at a lift coefficient of about 0·5 at a Mach number of 1·82.

Visual flow observations showed no signs of leading-edge separation within the incidence range of the tests. A photograph of surface oil flow at a Mach number of 1·61 and a lift coefficient of 0·48, with the leading edges of both wings roughened, is reproduced in Fig. 10. Between the leading edge and a line from near 10 per cent chord at the root to the trailing edge at 60 per cent exposed span, the surface flow was inclined inwards at an angle of about 20 deg to the vertical plane of symmetry of the model*, as a result of the acceleration round the leading edge of the flow component normal to it. The boundary on the wing of the inward-directed flow appears to have been the foot of a shock reducing the inclination to the plane of symmetry of the flow above the wing ; the surface flow near the wing root was chordwise, while close behind the shock the oil flowed parallel to or towards the shock, showing that at least a local separation occurred. The oil-flow pattern downstream of the shock bears a strong resemblance to that near the tip of the roughened wing in Fig. 7c. Again, a possible explanation of the pattern is that the boundary layer, separating at the foot of the shock, formed a vortex sheet which rolled up in sections to produce an array of streamwise vortices close above the wing surface. Stanbrook has reported in Ref. 14 an array of vortices produced by the interaction of a wing-root leading-edge shock with the boundary layer on the body of a wing-body combination ; there, as in the present case, the line of intersection of the shock with the surface on which the interaction took place was swept back relative to the local flow direction.

The angle of sweep of the foot of the shock increased with Mach number at a constant angle of incidence.

There was a small area of complete separation at the trailing edge between 45 per cent and 65 per cent exposed span, where the oil flow had a forward component. The trailing-edge shock appeared to have moved forward locally on to the wing at its intersection with the swept shock. The extent of the separation was not easy to determine ; it grew rapidly at the tip as the Reynolds number fell while the tunnel pressure was being reduced before shutting down. An azobenzene sublimation test confirmed that the area of separation was small. It may be speculated that the variation with Mach number of the lift coefficient at which the aerodynamic centre began to move forward was related to the development of this separation, but no definite evidence to support such a conclusion has been obtained.

4. *Concluding Remarks.*—In this paper some features of the lift and stability characteristics of a delta-winged model have been analysed in a tentative way, with the help of surface oil-flow observations.

At Mach numbers up to at least $1 \cdot 07$ there was a boundary-layer separation from the leading edge of the wing at incidence, forming a vortex sheet with its free edge rolled up above the wing. The effects of the vortex sheet on lift and stability at Mach numbers up to $0 \cdot 8$ were qualitatively similar to what has been observed at low speeds on other wings. At Mach numbers close below $1 \cdot 0$, an interaction between the leading-edge vortex sheet and the shock near the trailing edge on the upper surface caused unsteadiness of the loading of the wing at lift coefficients greater than $0 \cdot 6$, and at a Mach number of $0 \cdot 99$ a severe pitch-up at a lift coefficient of about $0 \cdot 9$. An aircraft with a thicker wing of similar plan-form, or, more generally, an aircraft of such a configuration that a strong shock is formed across a swept wing with a leading-edge vortex sheet at high subsonic speeds, might experience similar undesirable effects at lower lift coefficients and Mach numbers.

At Mach numbers between $1 \cdot 42$ and $1 \cdot 82$ the boundary layer remained attached at the leading edge in the incidence range of the tests, and an oblique shock lay across the upper surface of the wing at incidence from near the root leading edge. There was a small area of shock-induced separation at the trailing edge of the wing. Relatively small changes in stability with variation of lift coefficient were observed at these Mach numbers.

Acknowledgement.—The author is indebted to Mr. J. B. Scott-Wilson for the surface oil-flow photographs in Figs. 6 and 7.

* In this region the oil flowed only in patches and very slowly, along closely spaced fine lines. The lines were also found in an azobenzene sublimation pattern, where they closely resembled the traces of fine vortices due to the instability of a laminar boundary layer, reported by Scott-Wilson and Capps in Ref. 13. Nevertheless, the nature of the interaction of the boundary layer with the shock appeared typical of a turbulent boundary layer, while an interaction of the type usually associated with laminar boundary layers appeared to occur when the leading edge was not roughened.

LIST OF SYMBOLS

$\bar{\bar{c}}$	Aerodynamic mean chord
M	Mach number
q	Free-stream dynamic pressure
R	Reynolds number based on aerodynamic mean chord
S	Gross wing area
α	Angle of incidence
C_L	Lift coefficient $\equiv \frac{\text{lift}}{qS}$
C_m	Pitching-moment coefficient $\equiv \frac{\text{pitching moment}}{qS\bar{\bar{c}}}$ referred to mean quarter-chord point

REFERENCES

No.	*Author*	*Title, etc.*
1	D. E. Morris	Calibration of the flow in the working-section of the 3-ft × 3-ft Wind Tunnel, National Aeronautical Establishment. C.P. 261. September, 1954.
2	E. P. Sutton	The development of slotted working-section liners for transonic operation of the R.A.E. (Bedford) 3-ft Wind Tunnel. R. & M. 3085. March, 1955.
3	K. G. Winter, J. B. Scott-Wilson and F. V. Davies	Methods of determination and of fixing of boundary-layer transition on wind-tunnel models at supersonic speeds. C.P. 212. September, 1954.
4	F. O'Hara and J. B. Scott-Wilson	An investigation of the flow on a half-wing model with 60·5 deg leading-edge sweepback at a high subsonic and supersonic speeds. C.P. 471. November, 1955.
5	M. Roy	Caractères de l'écoulement autour d'une aile en flèche accentuée. Comptes Rendus de l'Académie des Sciences. 234. p. 2501. June, 1952.
6	D. Küchemann	The effects of viscosity on the type of flow on swept wings. Paper 5, Proceedings of Symposium on Boundary-Layer Effects in Aerodynamics, National Physical Laboratory. March/April, 1955.
7	D. Küchemann	A non-linear lifting-surface theory for wings of small aspect ratio with edge separations. A.R.C. 17769. April, 1955.
8	E. C. Maskell	Flow separation in three dimensions. A.R.C. 18063. November, 1955.
9	A. B. Haines	Some notes on the flow patterns observed over various swept-back wings at low Mach number (in the R.A.E. 10-ft × 7-ft High-Speed Tunnel). A.R.C. 17067. September, 1954.
10	N. C. Lambourne and P. S. Pusey	Some visual observations of the flow over a swept-back wing in a water tunnel, with particular reference to high incidences. C.P. 192. May, 1954.
11	K. Orlik-Rückemann	Experimental determination of pressure distributions and transition lines of plane delta wings at low speeds and zero yaw. Royal Institute of Technology, Stockholm. KTH-Aero. Tech. Note 3. 1948.
12	A. E. Anderson	Chordwise and spanwise loadings measured at low speed on large triangular wings. N.A.C.A. Research Memo. A9 B17, NACA/TIB/2109. April, 1949.
13	J. B. Scott-Wilson and D. S. Capps	Wind-tunnel observations of boundary-layer transition on two swept-back wings at a Mach number of 1·61. A.R.C. 17627. December, 1954.
14	A. Stanbrook	Experimental observation of vortices in wing-body junctions. R. & M. 3114. March, 1957.
15	D. H. Peckham	Low-speed wind-tunnel tests on a series of uncambered slender pointed wings with sharp edges. R. & M. 3186. December, 1958.

TABLE 1

Numerical Values of Lift and Pitching-Moment Coefficients

M	α (deg)	C_L	C_m
0·70	− 1·06	−0·051	+0·0064
	− 0·53	−0·024	0·0039
	+ 0·01	+0·004	+0·0008
	0·55	0·032	−0·0022
	1·07	0·060	−0·0049
	2·14	0·116	−0·0108
	3·20	0·172	−0·0166
	4·27	0·232	−0·0232
	5·34	0·290	−0·0291
	6·40	0·347	−0·0342
	7·47	0·406	−0·0383
	8·53	0·462	−0·0406
	9·60	0·512	−0·0389
	10·65	0·557	−0·0420
	11·72	0·610	−0·0471
	12·80	0·669	−0·0548
	+13·86	+0·719	−0·0590
0·80	− 1·09	−0·057	+0·0077
	− 0·54	−0·027	0·0043
	+ 0·01	+0·003	+0·0005
	0·54	0·034	−0·0031
	1·08	0·064	−0·0064
	1·62	0·095	−0·0098
	2·16	0·125	−0·0134
	3·23	0·187	−0·0210
	4·32	0·248	−0·0279
	5·39	0·308	−0·0340
	6·47	0·368	−0·0391
	7·54	0·423	−0·0420
	8·62	0·477	−0·0406
	9·69	0·525	−0·0442
	10·74	0·572	−0·0500
	11·82	0·627	−0·0578
	12·90	0·689	−0·0678
	+13·97	+0·741	−0·0750
0·90	− 1·08	−0·061	+0·0091
	− 0·54	−0·028	0·0048
	+ 0·01	+0·004	+0·0004
	0·55	0·038	−0·0042
	1·10	0·071	−0·0086
	2·19	0·137	−0·0175
	3·28	0·205	−0·0264
	4·37	0·270	−0·0345
	5·46	0·333	−0·0418
	6·55	0·398	−0·0499
	7·63	0·458	−0·0563
	8·72	0·517	−0·0605
	9·25	0·543	−0·0639
	9·79	0·567	−0·0655
	10·85	0·606	−0·0684
	11·92	0·659	−0·0784
	13·00	0·716	−0·0913
	+14·07	+0·768	−0·1006
0·93	− 1·08	−0·063	+0·0098
	+ 0·01	+0·005	+0·0004
	1·10	0·073	−0·0093
	2·20	0·143	−0·0195
	4·39	0·281	−0·0402
	6·57	0·408	−0·0577
	7·66	0·472	−0·0659
	8·73	0·524	−0·0703
	9·82	0·583	−0·0768
	10·89	0·635	−0·0817
	11·96	0·676	−0·0872
	13·04	0·726	−0·0977
	+14·12	+0·775	−0·1091
0·96	− 1·09	−0·070	+0·0143
	+ 0·01	+0·006	+0·0001
	1·12	0·082	−0·0142
	2·22	0·160	−0·0288
	3·32	0·233	−0·0432
	4·42	0·302	−0·0547
	5·51	0·367	−0·0639
	6·59	0·425	−0·0711
	7·69	0·488	−0·0800
	8·78	0·551	−0·0897
	9·88	0·618	−0·0993
	10·96	0·670	−0·1018
	12·03	0·710	−0·1033
	13·10	0·755	−0·1100
	+14·19	+0·809	−0·1219
1·02	− 1·09	−0·064	+0·0150
	+ 0·01	+0·009	−0·0016
	1·12	0·083	−0·0187
	2·22	0·159	−0·0360
	4·43	0·310	−0·0698
	6·64	0·449	−0·0953
	7·75	0·520	−0·1068
	8·85	0·591	−0·1193
	9·96	0·662	−0·1335
	11·07	0·732	−0·1470
	12·17	0·795	−0·1583
	13·27	0·856	−0·1692
	+14·36	+0·912	−0·1781

TABLE 1—*continued*

M	α (deg)	C_L	C_m	M	α (deg)	C_L	C_m
0·99	− 1·09	−0·070	+0·0169	1·61	− 3·51	−0·166	+0·0369
	− 0·54	−0·031	0·0078		− 2·43	−0·118	0·0266
	+ 0·01	+0·004	+0·0003		− 1·38	−0·068	0·0155
	0·56	0·046	−0·0094		− 0·32	−0·016	+0·0040
	1·11	0·083	−0·0181		+ 0·74	+0·033	−0·0070
	1·66	0·122	−0·0270		1·81	0·085	−0·0182
	2·21	0·162	−0·0359		2·87	0·133	−0·0287
	3·32	0·239	−0·0538		3·93	0·184	−0·0398
	3·87	0·279	−0·0630		4·99	0·232	−0·0500
	4·41	0·314	−0·0700		6·06	0·281	−0·0602
	5·51	0·382	−0·0810		7·13	0·337	−0·0717
	6·05	0·416	−0·0862		8·19	0·383	−0·0813
	6·61	0·447	−0·0909		9·25	0·429	−0·0902
	7·70	0·519	−0·1047		10·31	0·477	−0·1002
	8·80	0·586	−0·1148		11·38	0·523	−0·1097
	9·88	0·641	−0·1209		12·44	0·569	−0·1192
	10·99	0·713	−0·1322		+13·50	+0·615	−0·1279
	11·54	0·749	−0·1421				
	12·11	0·802	−0·1567	1·82	− 4·20	−0·178	+0·0381
	13·20	0·866	−0·1689		− 3·15	−0·136	0·0292
	13·74	0·886	−0·1685		− 2·10	−0·090	0·0198
	+14·23	+0·859	−0·1431		− 1·05	−0·048	0·0103
					+ 0·00	−0·005	+0·0010
1·42	− 2·24	−0·120	+0·0259		1·04	+0·035	−0·0080
	− 0·11	−0·006	+0·0006		2·09	0·079	−0·0171
	+ 2·02	+0·100	−0·0244		3·14	0·124	−0·0266
	4·16	0·211	−0·0488		4·19	0·168	−0·0355
	5·23	0·267	−0·0612		5·24	0·209	−0·0439
	6·30	0·323	−0·0733		6·29	0·252	−0·0525
	7·37	0·378	−0·0851		7·34	0·295	−0·0611
	+ 8·43	+0·429	−0·0948		8·39	0·338	−0·0687
					9·44	0·377	−0·0760
					10·49	0·417	−0·0835
					11·54	0·458	−0·0910
					12·59	0·495	−0·0975
					13·64	0·533	−0·1038
					+14·70	+0·571	−0·1089

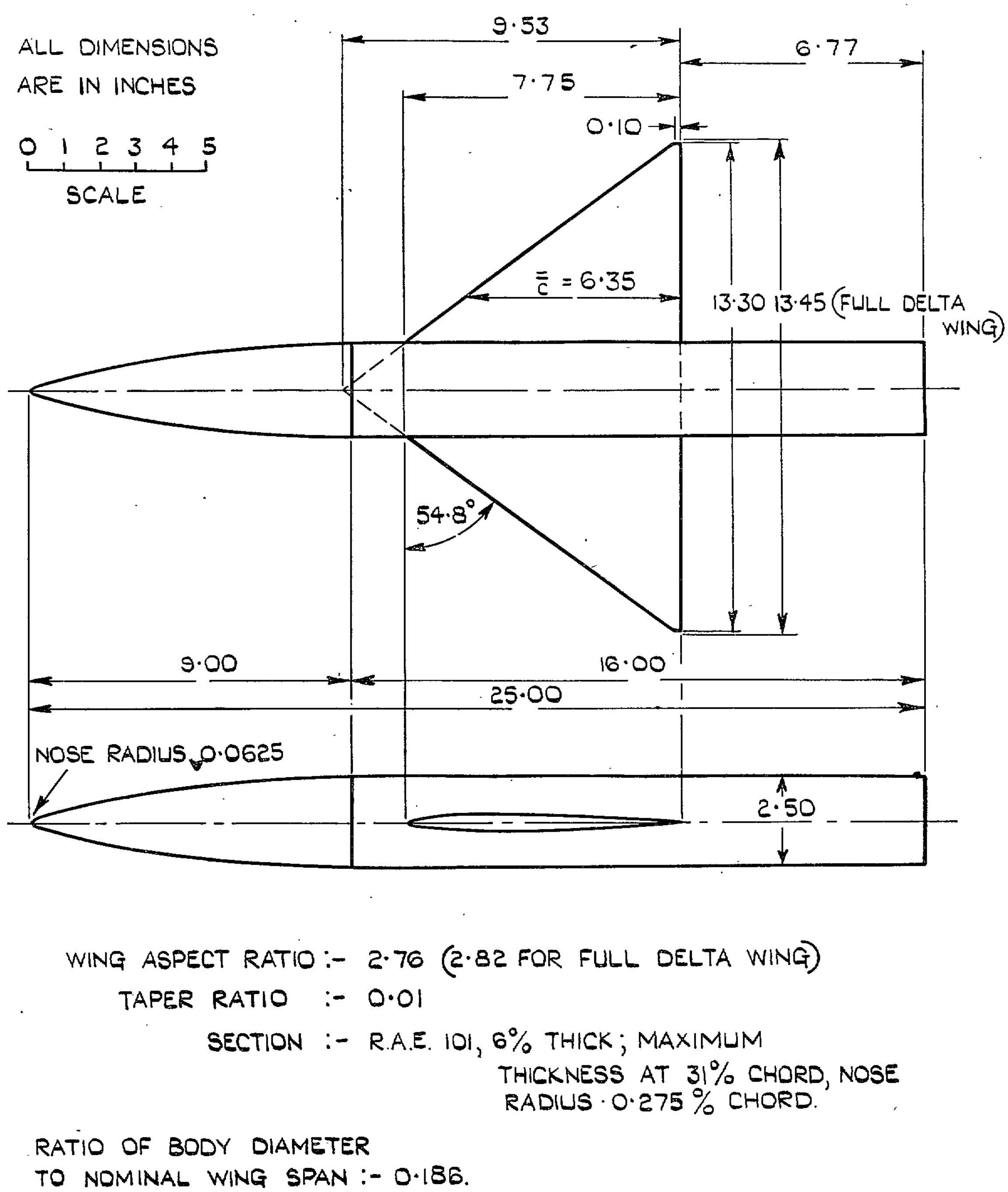

FIG. 1. Dimensions of the model.

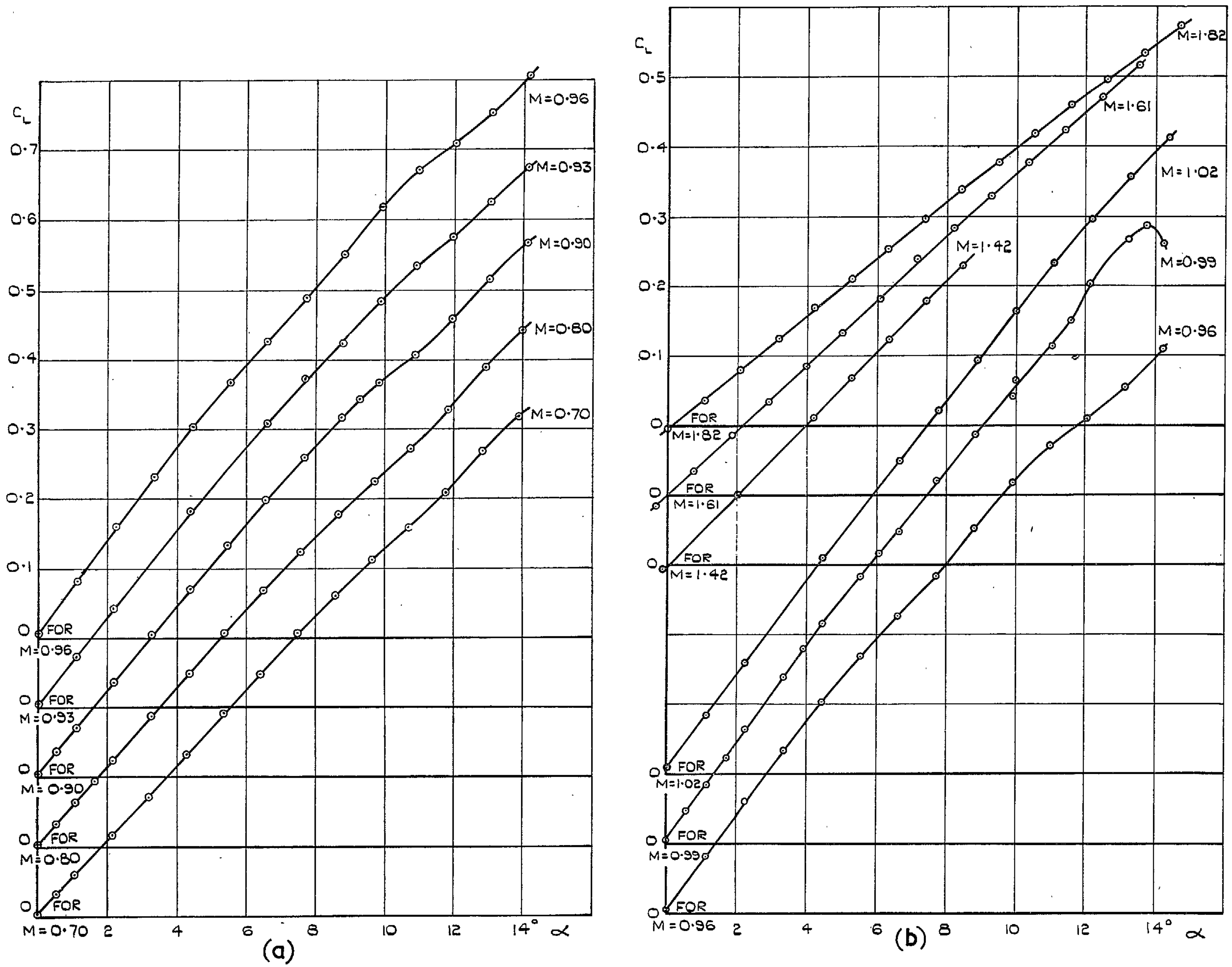

FIGS. 2a and 2b. Variation of lift with incidence.

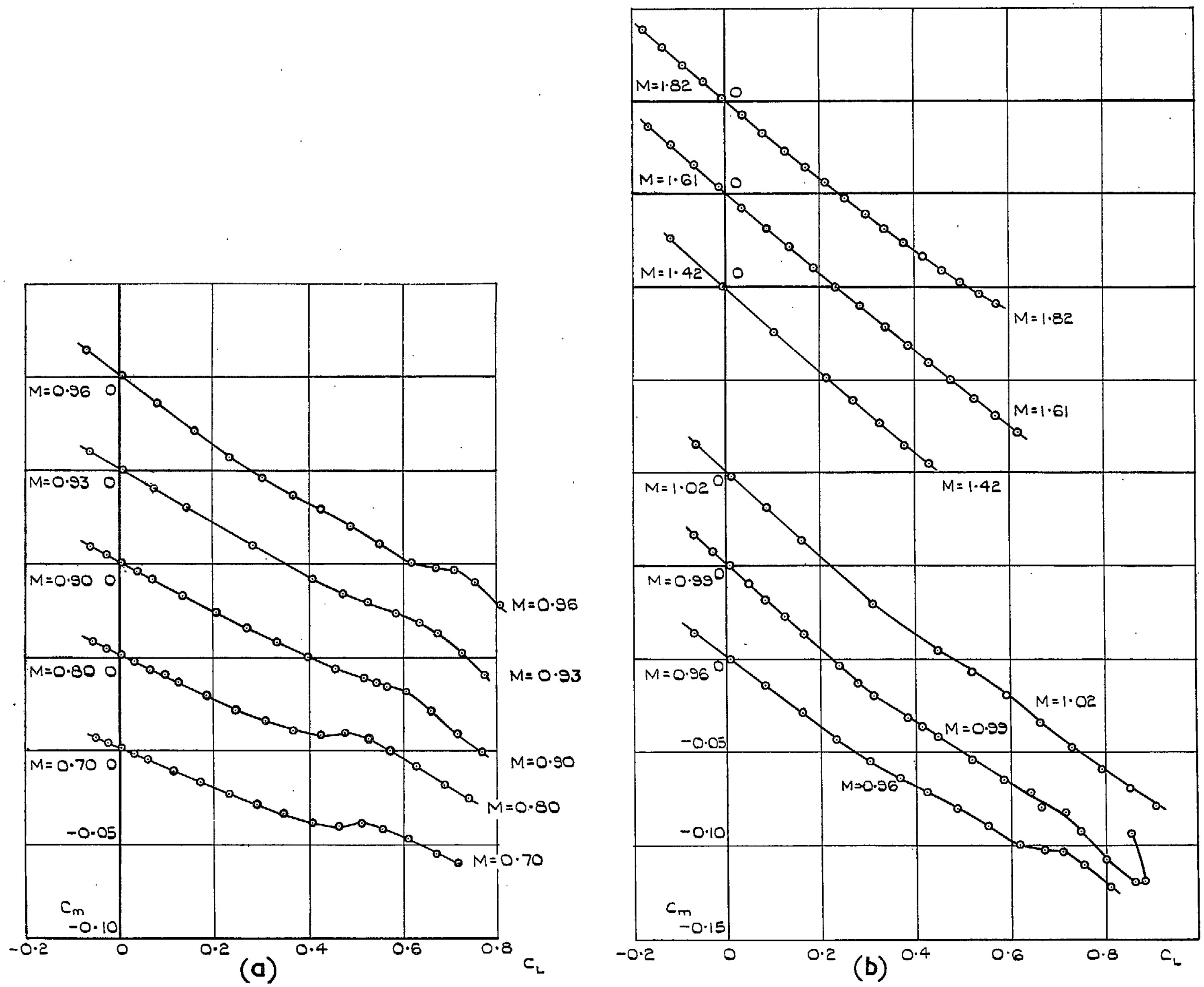

FIGS. 3a and 3b. Variation of pitching moment with lift.

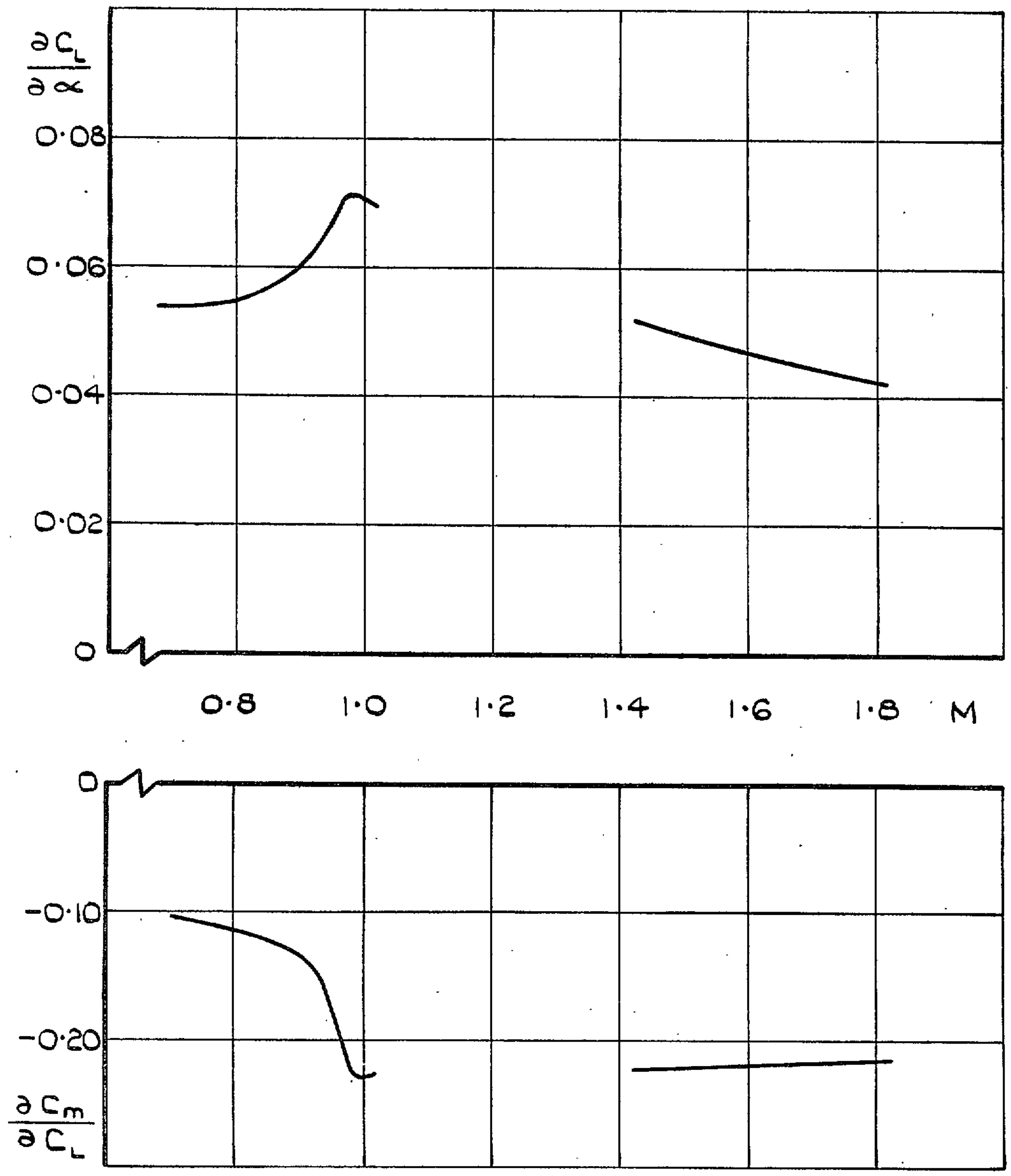

FIG. 4. Variation of lift-curve slope and aerodynamic-centre position at zero lift with Mach number.

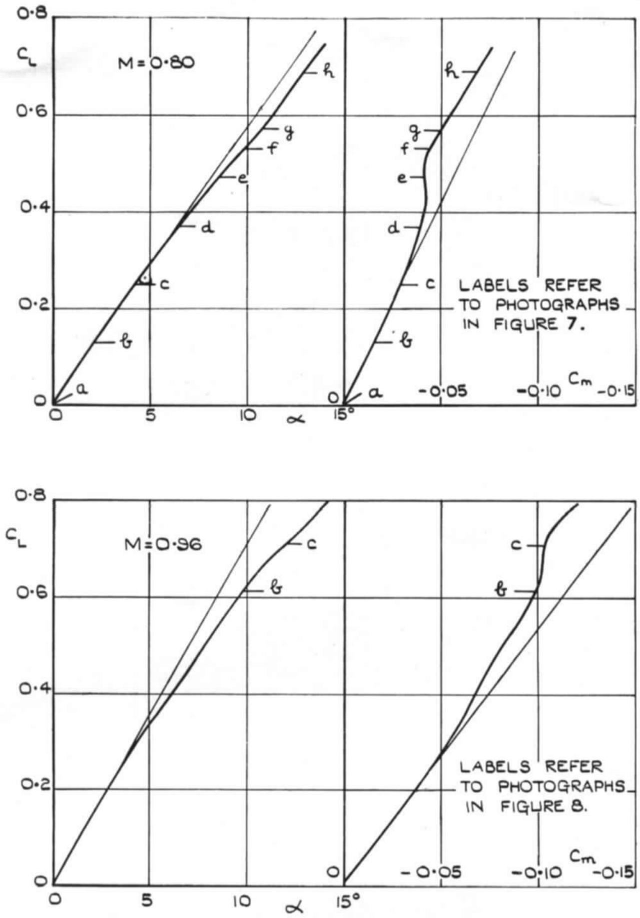

FIG. 5. Lift and stability at Mach numbers of 0·80 and 0·96.

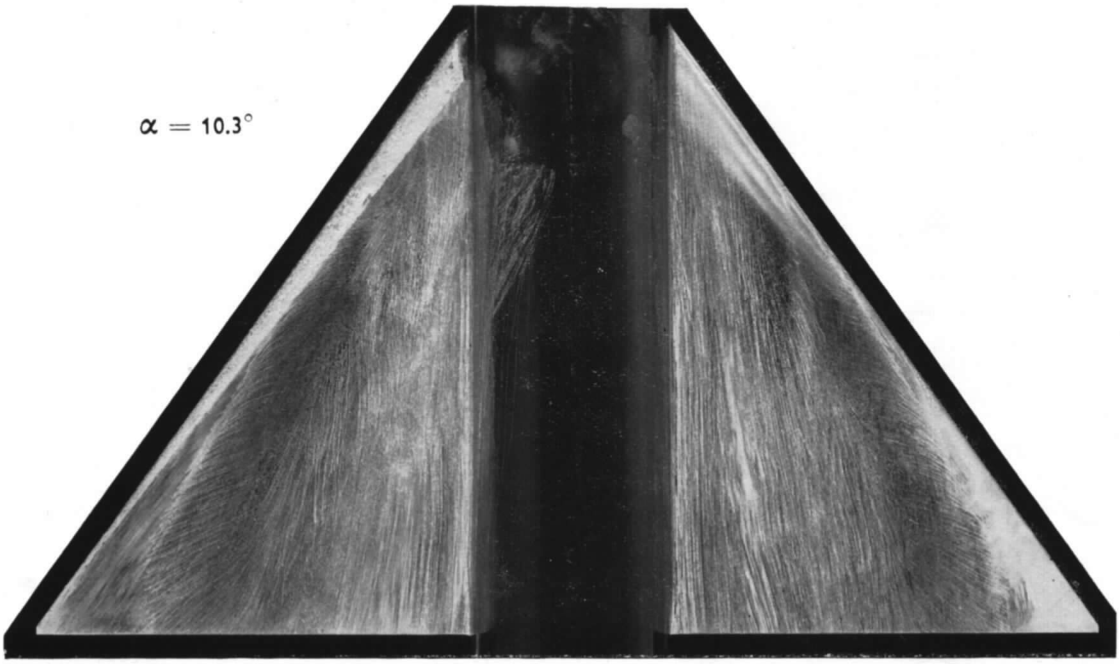

FIG. 6. Surface oil flow at a Mach number of 0·40.

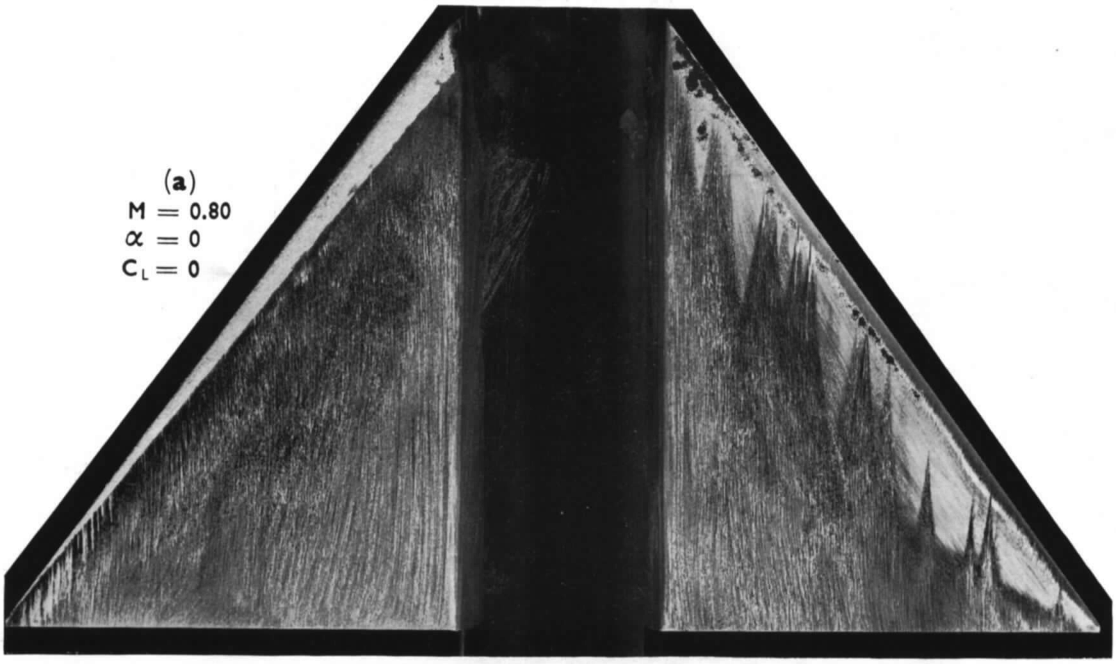

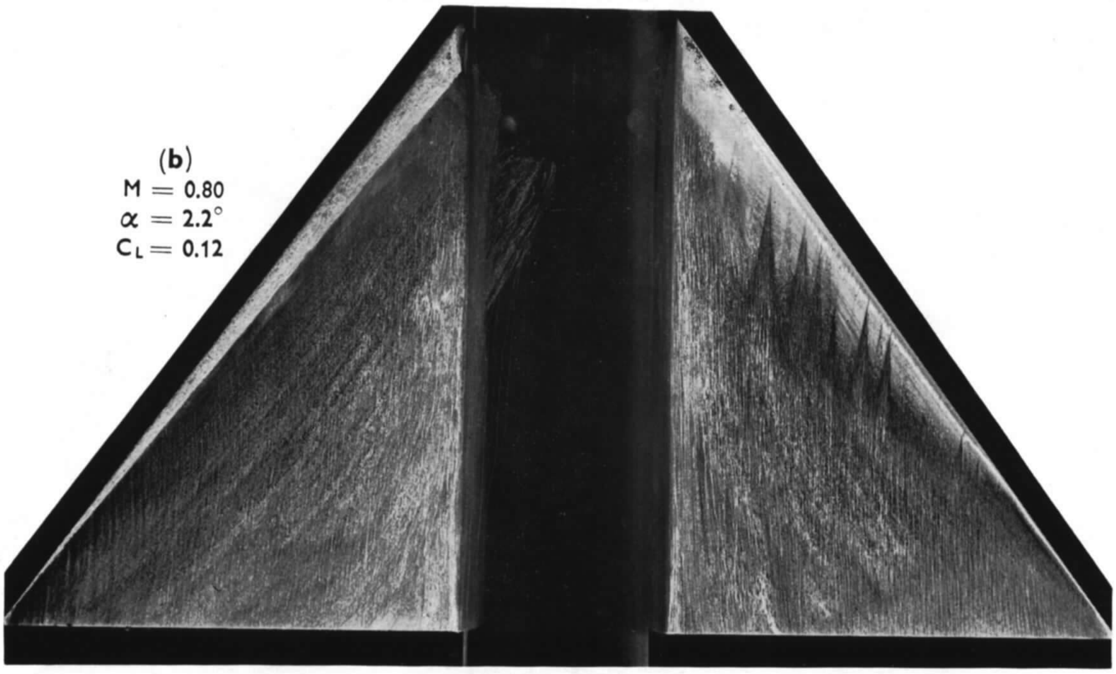

FIGS. 7a and 7b. Surface oil flow at a Mach number of 0·80.

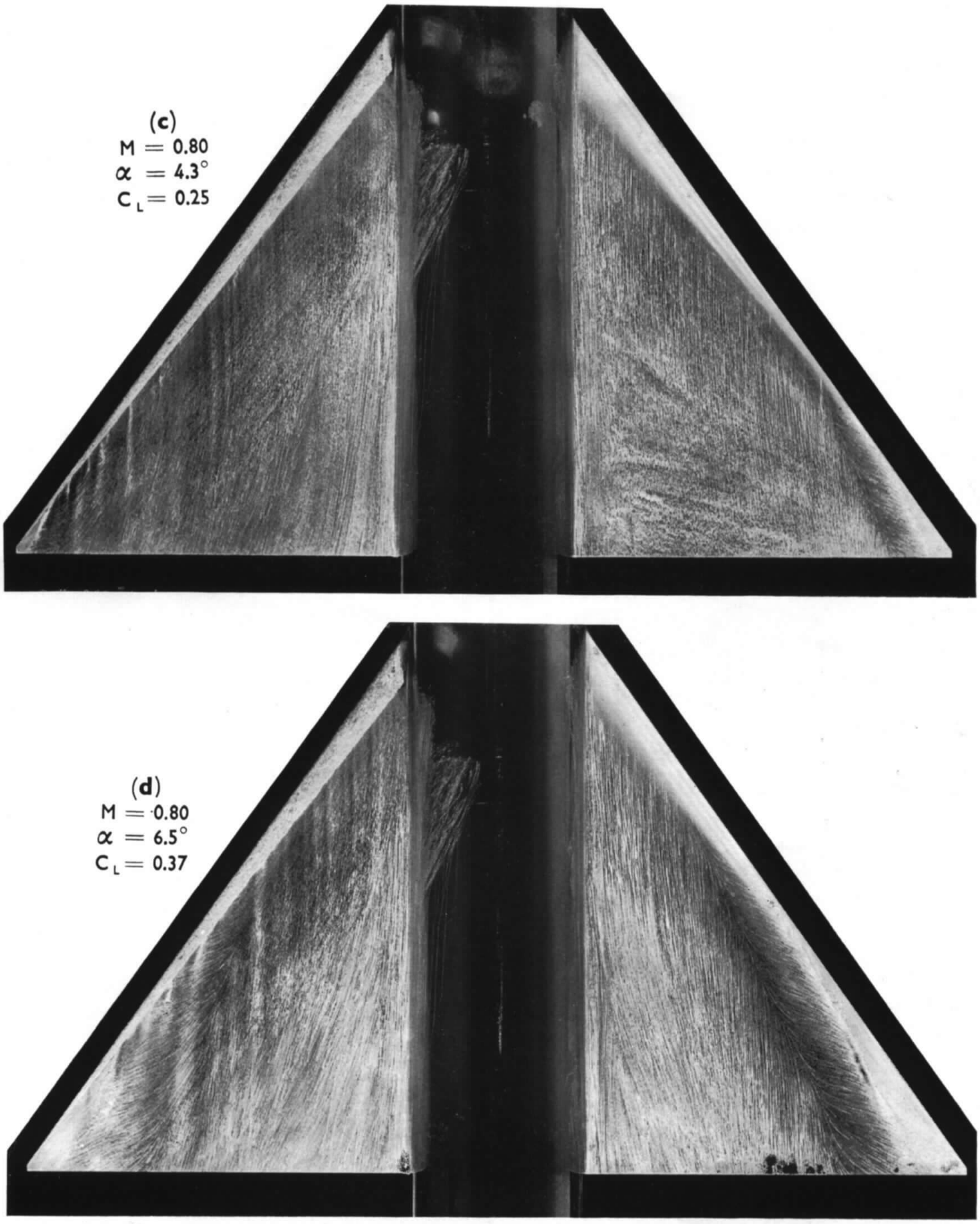

FIGS. 7c and 7d. Surface oil flow at a Mach number of 0·80.

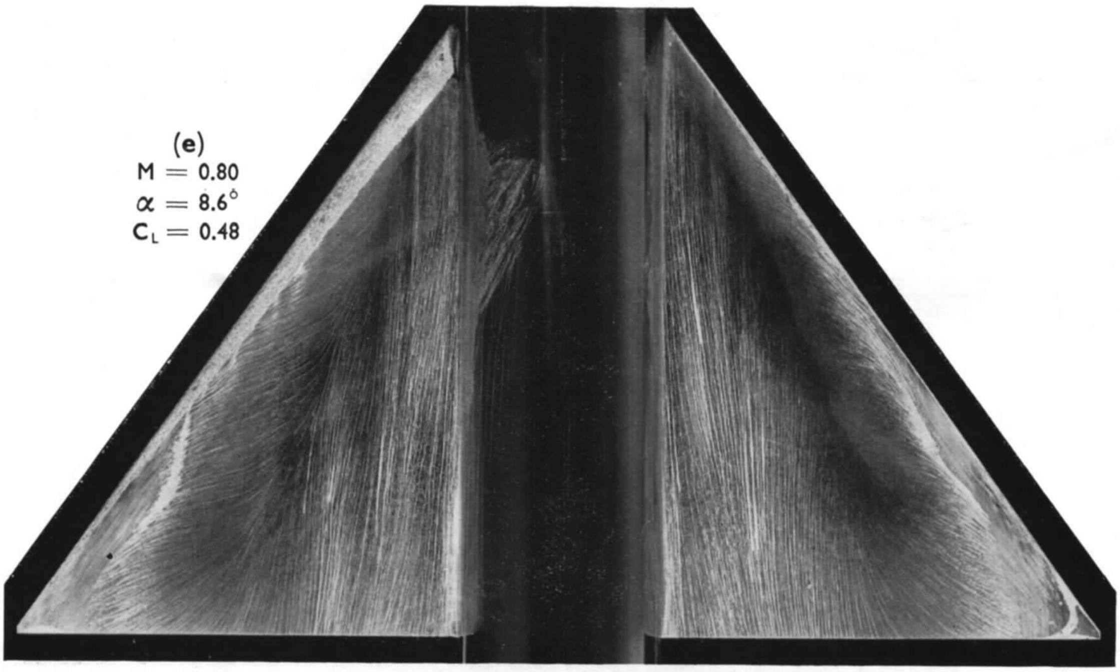

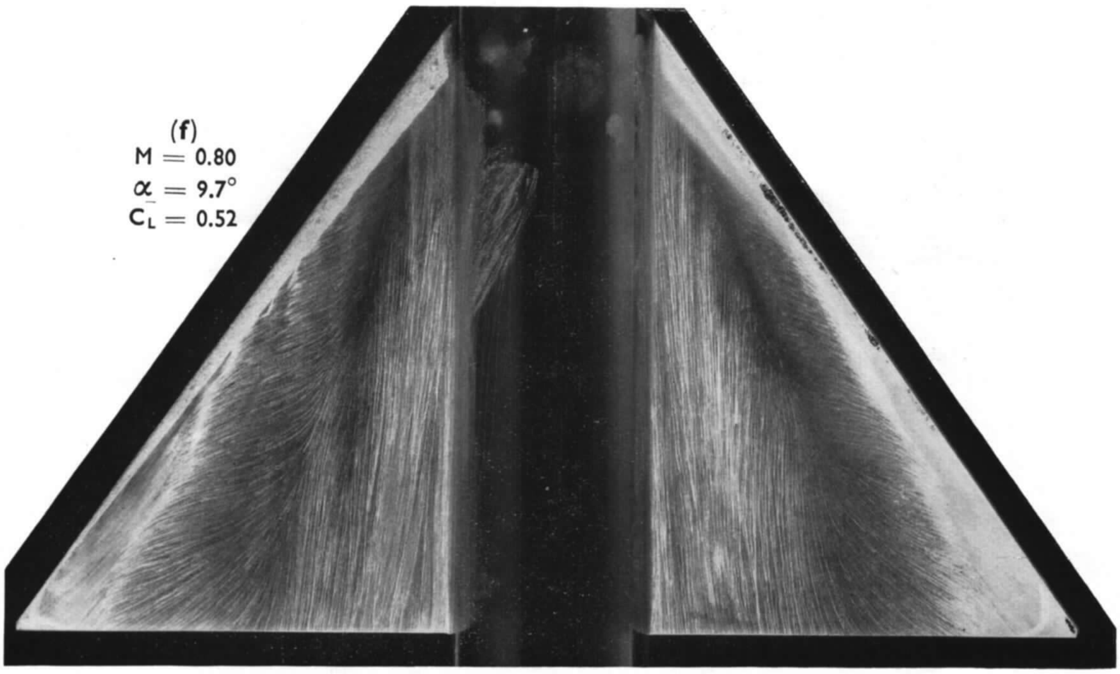

FIGS. 7e and 7f. Surface oil flow at a Mach number of 0·80.

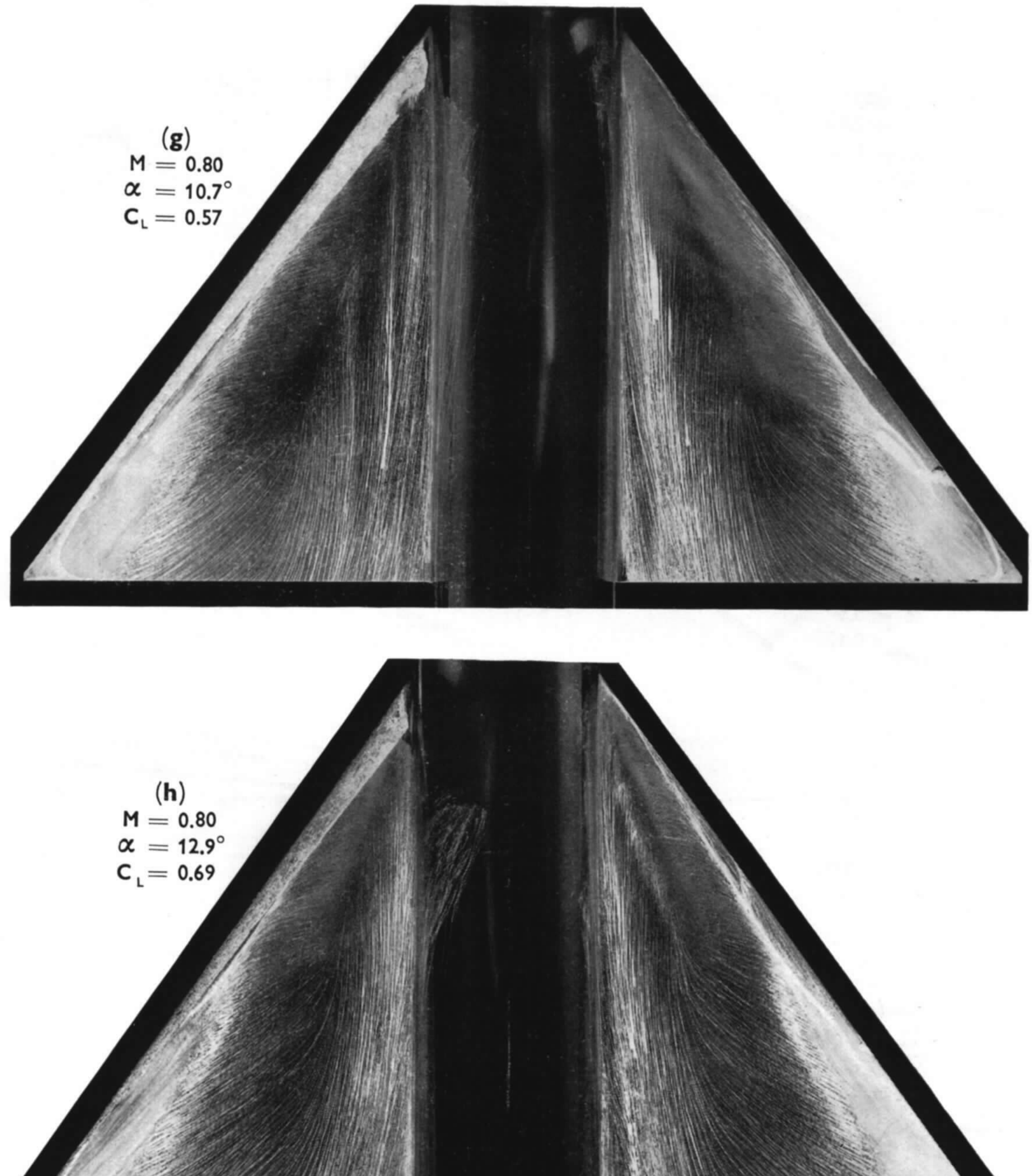

FIGS. 7g and 7h. Surface oil flow at a Mach number of 0·80.

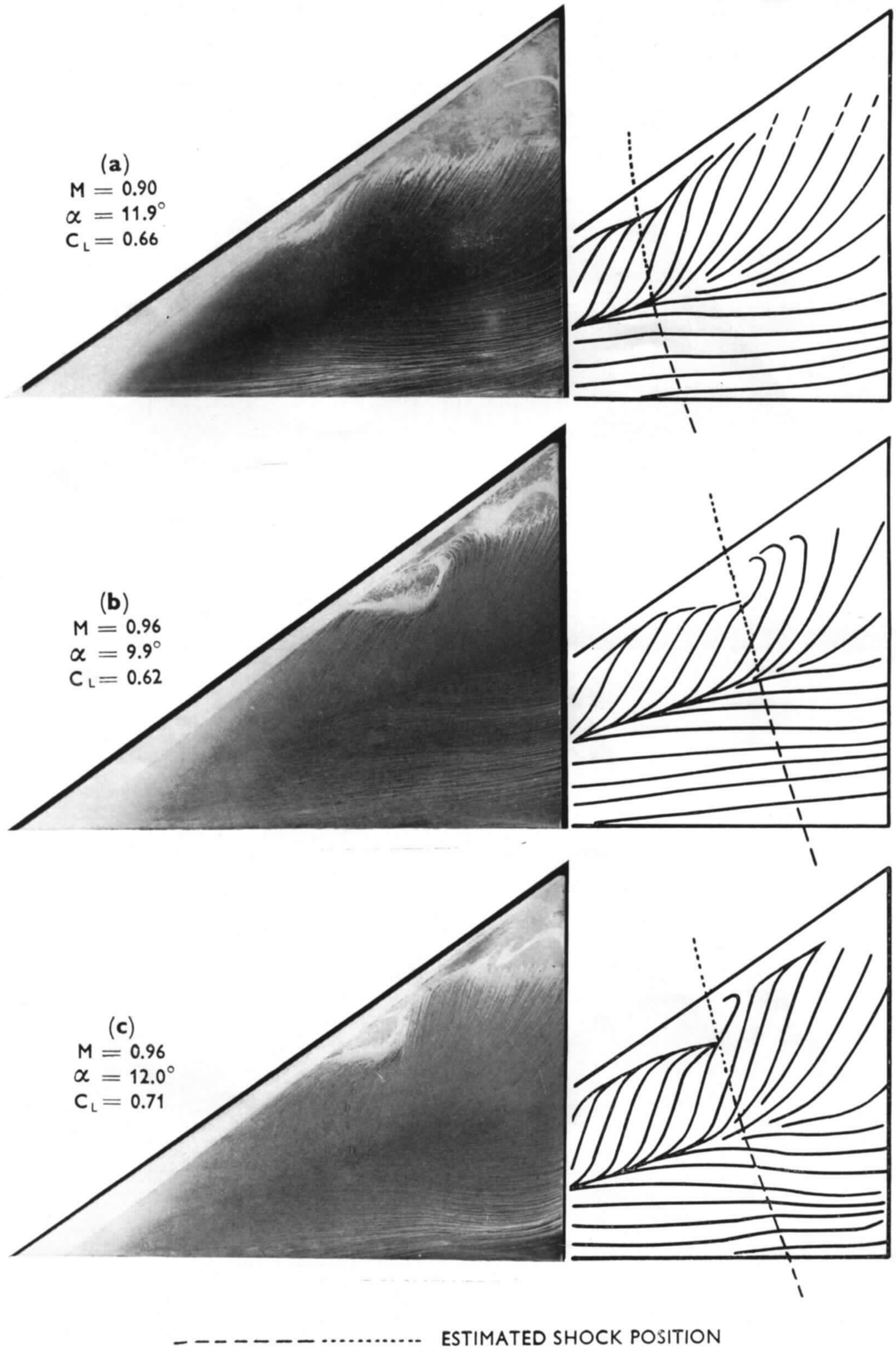

FIGS. 8a to 8c. Surface oil flow at Mach numbers of 0·90 and 0·96.

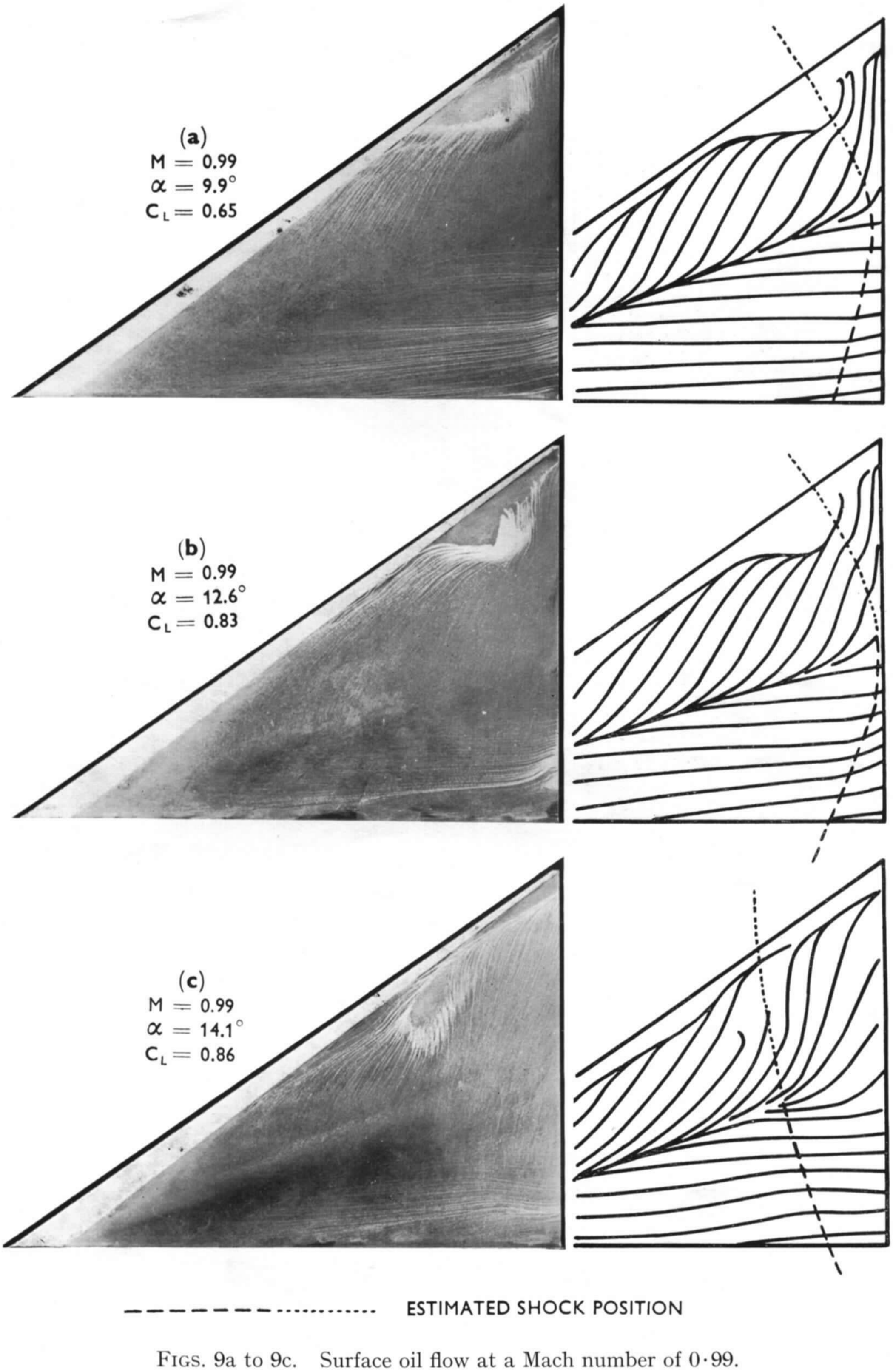

FIGS. 9a to 9c. Surface oil flow at a Mach number of 0·99.

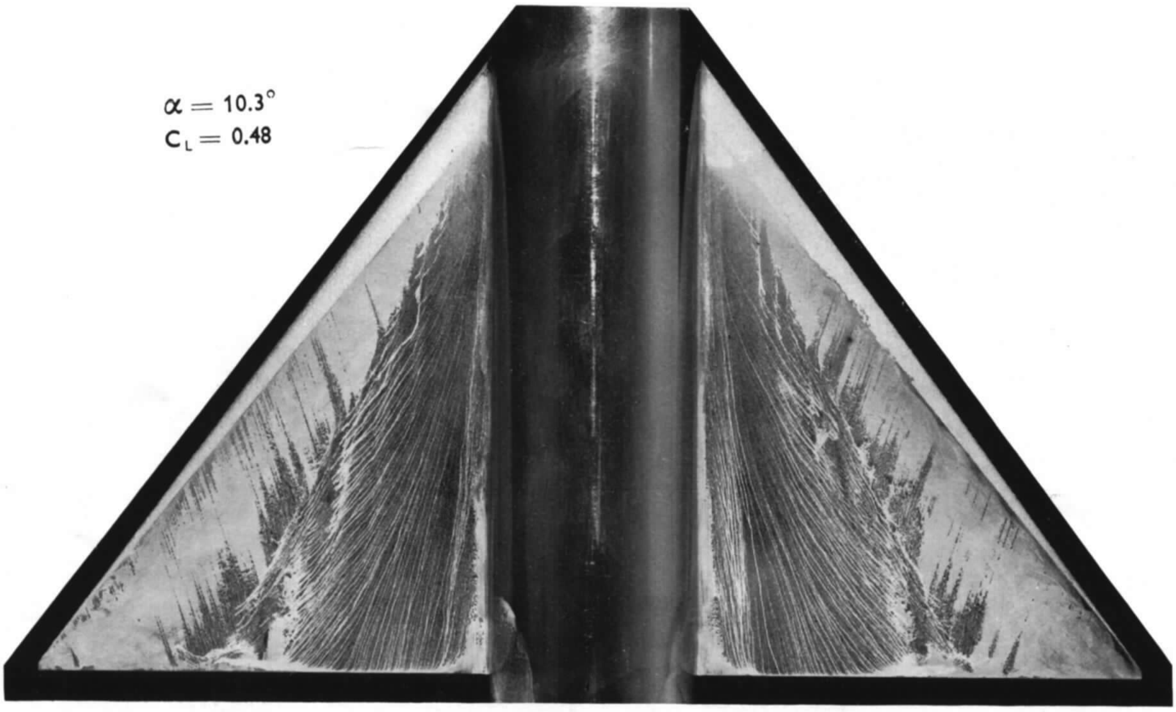

FIG. 10. Surface oil flow at a Mach number of $1 \cdot 61$.

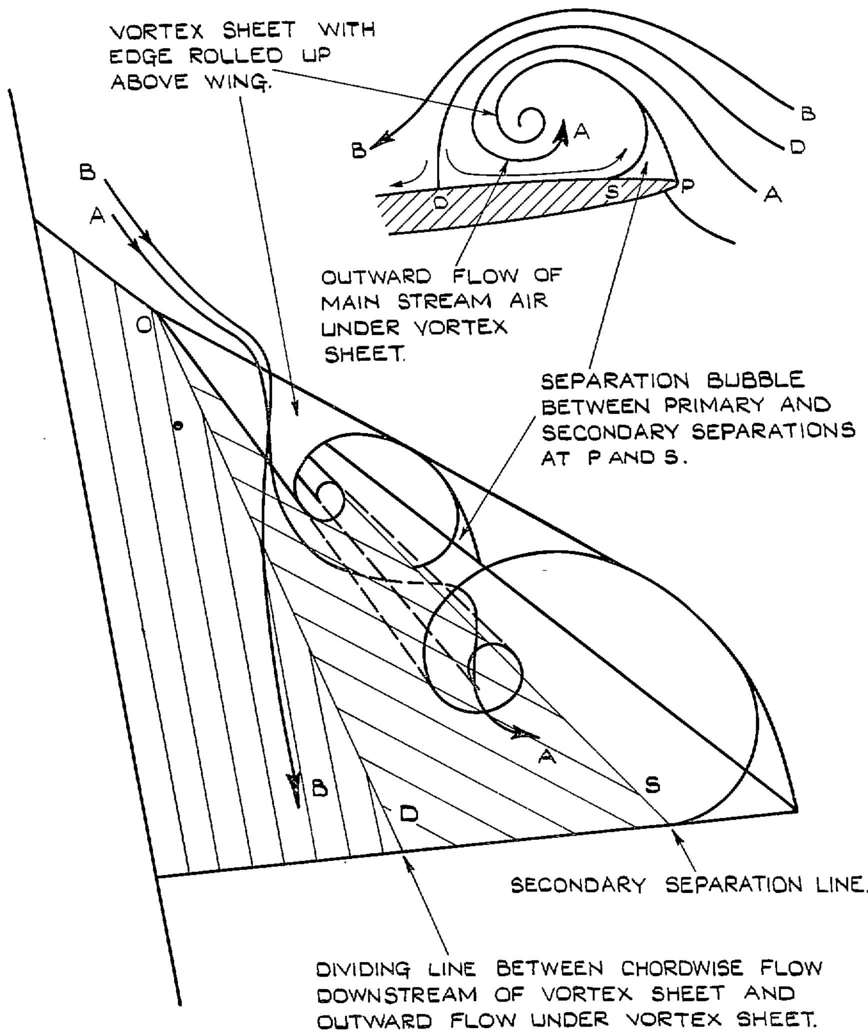

Fig. 11. Sketch of main features of flow with leading-edge separation and vortex sheet.

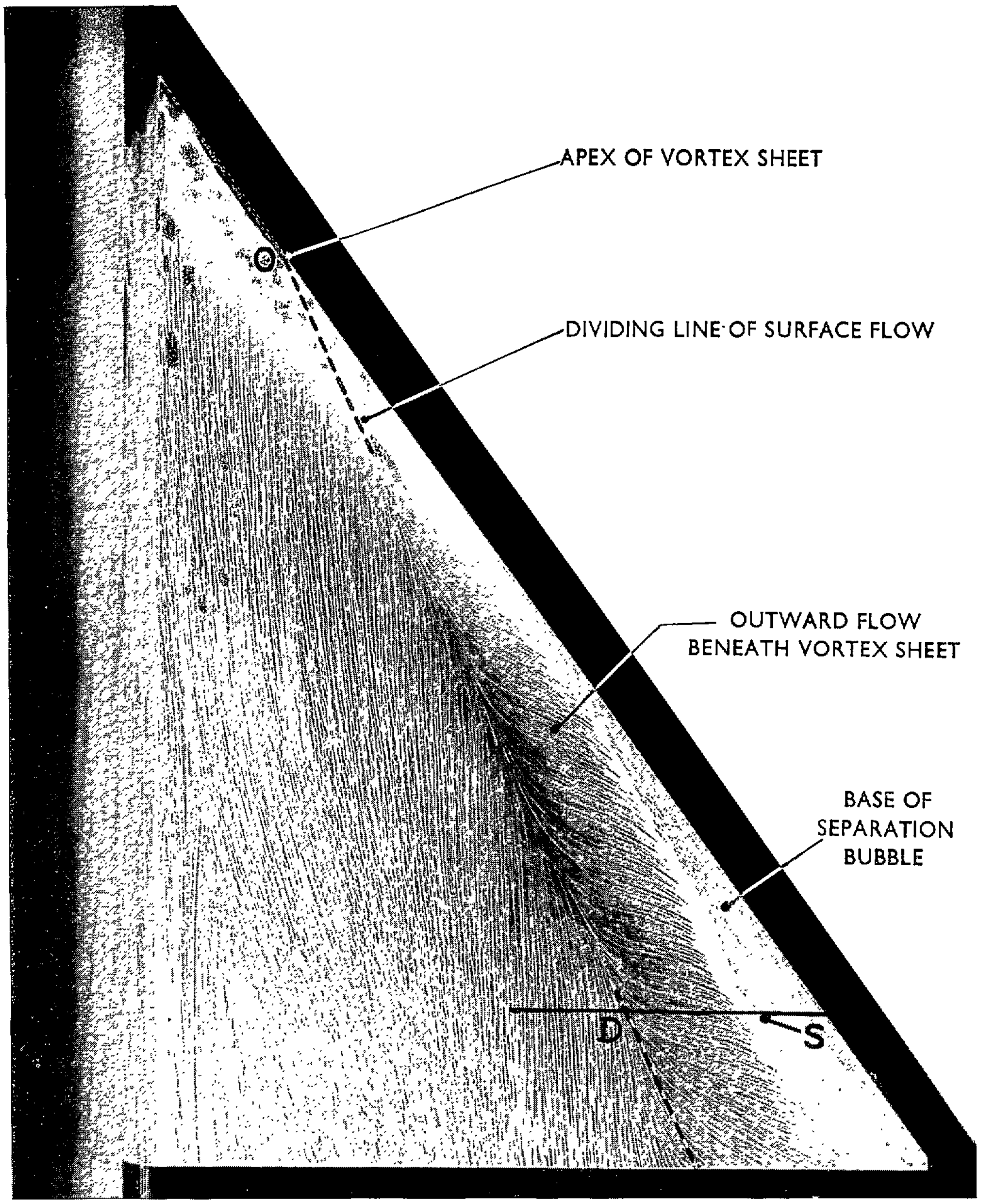

FIG. 12. Typical oil-flow pattern on wing with leading-edge vortex sheet at moderate incidence.

(80315) Wt. 61/991 K 7 12/60 Hw. PRINTED IN ENGLAND

Publications of the Aeronautical Research Council

ANNUAL TECHNICAL REPORTS OF THE AERONAUTICAL RESEARCH COUNCIL (BOUND VOLUMES)

1939 Vol. I. Aerodynamics General, Performance, Airscrews, Engines. 50*s*. (52*s*.)
Vol. II. Stability and Control, Flutter and Vibration, Instruments, Structures, Seaplanes, etc. 63*s*. (65*s*.)

1940 Aero and Hydrodynamics, Aerofoils, Airscrews, Engines, Flutter, Icing, Stability and Control, Structures, and a miscellaneous section. 50*s*. (52*s*.)

1941 Aero and Hydrodynamics, Aerofoils, Airscrews, Engines, Flutter, Stability and Control, Structures. 63*s*. (65*s*. 3*d*.)

1942 Vol. I. Aero and Hydrodynamics, Aerofoils, Airscrews, Engines. 75*s*. (77*s*. 3*d*.)
Vol. II. Noise, Parachutes, Stability and Control, Structures, Vibration, Wind Tunnels. 47*s*. 6*d*. (49*s*. 3*d*.)

1943 Vol. I. Aerodynamics, Aerofoils, Airscrews. 80*s*. (82*s*.)
Vol. II. Engines, Flutter, Materials, Parachutes, Performance, Stability and Control, Structures. 90*s*. (92*s*. 3*d*.)

1944 Vol. I. Aero and Hydrodynamics, Aerofoils, Aircraft, Airscrews, Controls. 84*s*. (86*s*. 6*d*.)
Vol. II. Flutter and Vibration, Materials, Miscellaneous, Navigation, Parachutes, Performance, Plates and Panels, Stability, Structures, Test Equipment, Wind Tunnels. 84*s*. (86*s*. 6*d*.)

1945 Vol. I. Aero and Hydrodynamics, Aerofoils. 130*s*. (133*s*.)
Vol. II. Aircraft, Airscrews, Controls. 130*s*. (133*s*.)
Vol. III. Flutter and Vibration, Instruments, Miscellaneous, Parachutes, Plates and Panels, Propulsion. 130*s*. (132*s*. 9*d*.)
Vol. IV. Stability, Structures, Wind Tunnels, Wind Tunnel Technique. 130*s*. (132*s*. 9*d*.)

1947 Vol. I. Aerodynamics, Aerofoils, Aircraft. 168*s*. (171*s*. 3*d*.)

Annual Reports of the Aeronautical Research Council—

1939–48 3*s*. (3*s*. 5*d*.) 1949–54 5*s*. (5*s*. 5*d*.)

Index to all Reports and Memoranda published in the Annual Technical Reports, and separately—

April, 1950 - - - - - R. & M. 2600 6*s*. (6*s*. 2*d*.)

Published Reports and Memoranda of the Aeronautical Research Council—

Between Nos. 2351–2449	R. & M. No. 2450	2*s*. (2*s*. 2*d*.)
Between Nos. 2451–2549	R. & M. No. 2550	2*s*. 6*d*. (2*s*. 8*d*.)
Between Nos. 2551–2649	R. & M. No. 2650	2*s*. 6*d*. (2*s*. 8*d*.)
Between Nos. 2651–2749	R. & M. No. 2750	2*s*. 6*d*. (2*s*. 8*d*.)
Between Nos. 2751–2849	R. & M. No. 2850	2*s*. 6*d*. (2*s*. 8*d*.)
Between Nos. 2851–2949	R. & M. No. 2950	3*s*. (3*s*. 2*d*.)

Prices in brackets include postage

HER MAJESTY'S STATIONERY OFFICE

York House, Kingsway, London W.C.2; 423 Oxford Street, London W.1; 13a Castle Street, Edinburgh 2; 39 King Street, Manchester 2; 2 Edmund Street, Birmingham 3; 109 St. Mary Street, Cardiff; 50 Fairfax Street, Bristol 1; 80 Chichester Street, Belfast 1, *or through any bookseller.*

S.O. Code No. 23-3190

R. & M. No. 3190